Estuarine, Coastal and Shelf Science 301 (2024) 108726

Contents lists available at ScienceDirect

Estuarine, Coastal and Shelf Science

journal homepage: www.elsevier.com/locate/ecss

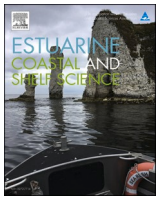

Beaches in a semi-insulated compartment: Engineering tools from the diffusion theory

Margherita Carmen Ciccaglione *, Mariano Buccino, Mario Calabrese

Department of Civil and Environmental Engineering, University of Naples Federico II, Via Claudio, 21, 80125, Naples, Italy

ARTICLE INFO

Keywords:
Shoreline evolution
Analytical modelling
Groin compartment
Coastal erosion
Bypass process

ABSTRACT

Beaches can serve as a valuable asset to any community, which can gain a massive source of income from them; in fact, beach tourism is ever more frequently the essential target of countries, aimed at attracting foreign investment or exchange. In this frame, prediction of coastal evolution at large scales is very important for coastal management and first conceptual design. Management strategies, almost at the early stages of the projects, **may** likely involve numerical simulations, but they can be extremely laborious, computing demanding and intensely time-consuming especially when involving either wider coastal domain or longer time scales that basically encompasses the majority of coastal projects by now. Analytical solutions of the Diffusion Shoreline Equation (DSE) can be a valid alternative. **I**n these frames, given the surprisingly good predictive capabilities, they can isolate essential features of the processes, making them more readily comprehended, and can avoid cumulative errors associated with the accuracy of computational time-stepping models. Nevertheless, the rather complex mathematical form makes their use extremely challenging and confines them in the realm of **high** mathematic**s**. Ciccaglione et al. (2023) provided analytical solutions of the DSE for finite beaches bounded by outcrops of whatever length (bypassing or non-bypassing groin compartments). Differently from the other studies, the authors checked the applicability range of the solutions through the comparison with reliable numerical models; furthermore, using curve fitting analysis simple design tools were suggested to aid engineers in the practical applications. In this paper, a deep focus is given on the case of a bypassing groin compartment, and easy-to-use formulae are given to assess the lifetime of beach fill projects. A simple semi-theoretical solution is also given for the case of a compartment bounded by a very short groin, by introducing a "convective term" modelled via a Heavy-side function, $H(x)$. The practical usefulness of this solution is proved through an application to the evolution of a real beach along Italy's Adriatic coast.

1. Introduction

Nowadays, management strategies of sandy coasts and marine environments are becoming increasingly crucial to protect coastal areas **in accordance** to ever more stringent economic and social constraints. In particular, a reliable forecast of future development of shorelines, even considering climate change, is needed to judiciously invest economic resources; suffice to say that if substantial money has been invested to nourish beaches, there is a considerable interest in determining how long they can be expected to last. Therefore, the fast comprehension of mid to long term shoreline evolution is needed to perform rational management strategies, properly design coastal structures, and consequently, develop effective adaptation plans to coastal hazards.

For mid-term prediction purposes, numerical models based on the One-Line Contour Equation (OLCE) are most frequently employed, already at the preliminary stages of the project. OLCE models are relatively fast and flexible computational tools that allow to account for various kinds of initial and boundary conditions, as well as the presence of structures of different types (Hanson and Kraus, 1989; Hanson et al., 2006; Reeve and Valsamidis, 2014; Di Paola et al., 2020; Buccino et al., 2020a, b, c; Ciccaglione et al., 2021).

Notwithstanding, computational time and drawbacks related to the spatial discretization of the coastline, can make numerical models unpractical, either when alternative solutions are most preliminarily compared or as a beach fill project is studied in a probabilistic frame. In those cases, theoretical solutions resulting from the Diffusion Shoreline Equation (DSE) can represent a valuable alternative.

DSE (e.g. Carslaw and Jaeger, 1959), is a fundamental **parabolic**

* Corresponding author.
E-mail addresses: margheritacarmen.ciccaglione@unina.it (M.C. Ciccaglione), buccino@unina.it (M. Buccino), mario.calabrese@unina.it (M. Calabrese).

https://doi.org/10.1016/j.ecss.2024.108726
Received 16 October 2023; Received in revised form 15 March 2024; Accepted 22 March 2024
Available online 24 March 2024

Partial Differential Equation (PDE), which governs heat conduction in solids and several other processes such as soil consolidation in geotechnics. Since the pioneering solution by Pelnard-Considere (1956), many researchers developed analytical tools for various contexts of application. Most of them, concerned with the hypothesis of open (unbounded) coast, which definitely simplifies the mathematical problem. The reader may refer to Larson et al. (1987) for a general review, and Dean (2003), for specific applications to the fields of beach nourishments and coastal management. Of particular interest for this research is the work published by Walton in 2005 (Walton, 2005), in which the author quantifies the bypass volume of a groin by means of the analytical solution of Pelnard-Considere (1956). Similarly, Reeve (2006) provided a full analytical solution, using the Fourier transform techniques, for the case of an impermeable isolated groin given a known arbitrary sequence of wave conditions and arbitrary source distribution; however, numerical integration over the arbitrary sequence of driving conditions was needed for the resolution. Then, Walton Jr and Dean (2011) presented closed-form solutions for piece-wise constant wave conditions at a groin; the piece-wise approach has been applied by Valsamidis et al. (2013) to a case study. Moreover, Valsamidis and Reeve (2017) developed solutions for the case of a beach between a groin and a river-mouth, accounting for the supply of sediment given by the river.

However, the unbounded coast assumption no longer holds true in a number of cases, such as many profitable and environmentally precious beaches along the Mediterranean coasts. Unfortunately, for these cases the solutions available are far less numerous. Larson et al. (1997) studied a single groin compartment, with no bypass, where the wave angle was allowed to vary seasonally; the method was subsequently simplified in the studies of Walton Jr and Dean (2011) and Valsamidis et al. (2013). Moreover, given the general solution of Reeve (2006) for a single groin, Zacharioudaki and Reeve (2008), extended the approach to an insulated groin compartment and obtained semianalytical solution to be performed through numerical integration to account for time varying wave conditions. Valsamidis and Reeve (2020) reworked the solution of Reeve (2006) and Zacharioudaki and Reeve (2008), to include the groin's permeability and provided a semi-analytical solution for an infinite groin field, subject to bypass. In the same year, Hoang (2020) came to a closed form solution for a beach bounded by groins of infinite length, which holds, however, only for wave attacks rigorously perpendicular to the coast. A common treat of those solutions is the rather complex mathematical form (often series of functions) that may confine them to the realm of pure mathematics, limiting their practical use.

Most recently, Ciccaglione et al. (2023) found a series of solutions of DSE that apply to finite beaches bounded by outcrops of **arbitrary** length (including zero-length). The method relies on the sum of two Sturm-Liouville Boundary Value Problems, which allow to account for both bypassing and non-bypassing conditions, as well as wave obliquity. Solutions are very simple, so they can be readily employed for the probabilistic design of artificial nourishments and, to a broader view, for the implementation of coastal management strategies.

As a point of novelty of the work, the analytical solutions were compared to the numerical outcomes of the OLCE-based software GENESIS (Hanson and Kraus, 1989), to assess whether they could hold even beyond their theoretical limitation of small angle. Furthermore, a curve fitting study was carried out to turn the solutions into simple easy-to-use formulae of practical interest; this essentially concerned in the remaining value of sediments in a beach fill of rectangular shape for a finite beach either pinned by revetments at the extremes or bounded by unbypassed groins (insulated beach).

In this study, we draw attention to a third solution of engineering interest from the Ciccaglione et al. approach, namely, a finite beach compartment bypassed on one side. After a review of the theoretical solution, in Section 2 we develop design tools for the 50% and 25% characteristic reduction times of a beach fill of rectangular shape. Subsequently (Section 3), we address the problem related to the presence of very short groins, which allow a significant amount of sand to enter or exit the compartment yet from the earliest evolution times. For those cases, we propose a physically consistent but not rigorous correction, based on the use of the Heavy-side function, $H(x)$. Finally, the reliability of the modified solution is checked against a case of real beach along the Adriatic coast of Italy.

2. Review of Ciccaglione et al. (2023) solution with a FOCUS ON the bypassed compartment

The planform evolution of a shoreline contour $y(x,t)$, is ruled by the One-Line Contour Equation (OLCE), originally introduced by Pelnard--Considere (1956). As is known, OLCE turns into the diffusivity equation (DSE) under the hypotheses of small breaking wave angle and mild shoreline curvature (Larson et al., 1987). DSE reads:

$$\frac{\partial y}{\partial t} = \varepsilon \frac{\partial^2 y}{\partial x^2} \tag{1}$$

where the parameter ε, (shoreline diffusivity) controls the speed at which the system responds to any external disturbance. ε is intensely dependent, above all, on the height and angle of breaking waves (H_b and θ_b) as described in many relationships in literature (Ashton and Murray, 2006a, b; Falqués, 2003; Falqués and Calvete, 2005; Walton and Dean, 2010).

Ciccaglione et al. (2023) assumes a beach of length L, bounded by two outcrops that protrude into the sea by $l_{h,1}$ and $l_{h,2}$, respectively (Fig. 1). For $t = 0$ the shoreline is approximately aligned to the x-axis ($y(0,0) \approx y(L,0) \approx 0$).

The shoreline function $y(x,t)$ is replaced by the quantity:

$$y' = y + \theta_b \cdot x \tag{2}$$

which also obeys to DSE. **The transformation selected for Eq. (2) primary allows to take into account for wave obliquity and aims to accommodate the natural rotation of the shoreline at the bounding outcrops, aligning it with the wave crest and thereby nullifying longshore sediment transport.** Subsequently, the bypassing boundary conditions at the extremes are set as follows:

$$\frac{\partial y'}{\partial x} l_{h,1} - y \bullet |\theta_b| = 0 \quad at\ x = 0 \tag{3a}$$

$$\frac{\partial y'}{\partial x} l_{h,2} + y \bullet |\theta_b| = 0 \quad at\ \ x = L \tag{3b}$$

and the evolution problem is finally split into the sum of two systems of differential equations in y', such that: $y' = y'_1 + y'_2$.

The first system represents the conduction of heat in a bar under Robin Boundary Conditions:

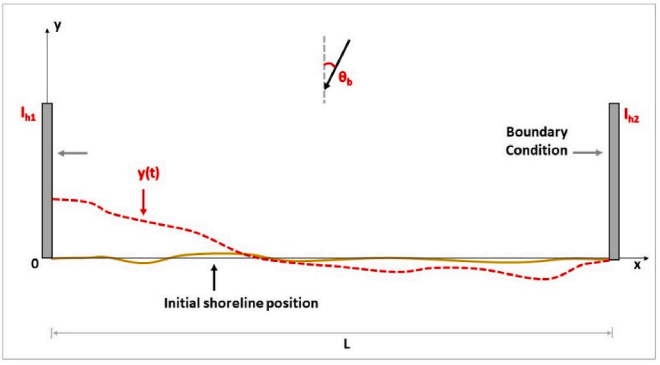

Fig. 1. Definition sketch for the evolution of a beach of finite length bounded by outcrops.

$$\frac{\partial y_1^{'}}{\partial t} - \varepsilon \frac{\partial^2 y_1^{'}}{\partial x^2} = 0 \quad t > 0; 0 \le x \le L \tag{4a}$$

$$\frac{\partial y_1^{'}}{\partial x} - \frac{y_1^{'} \bullet |\theta_b|}{l_{h,1}} = 0 \quad at \ x = 0 \tag{4b}$$

$$\frac{\partial y_1^{'}}{\partial x} + \frac{y_1^{'} \bullet |\theta_b|}{l_{h,2}} = 0 \quad at \ x = L \tag{4c}$$

$$y_1^{'}(x,0) = g^{'}(x) \tag{4d}$$

while the second is an Inhomogeneous Neumann Boundary Problem:

$$\frac{\partial y_2^{'}}{\partial t} - \varepsilon \frac{\partial^2 y_2^{'}}{\partial x^2} = 0 \quad t > 0; 0 \le x \le L \tag{5a}$$

$$\frac{\partial y_2^{'}}{\partial x} = 0 \quad at \ x = 0 \tag{5b}$$

$$\frac{\partial y_2^{'}}{\partial x} - \frac{\theta_b \bullet |\theta_b| L}{l_{h,2}} = 0 \quad at \ x = L \tag{5c}$$

The general form of the solution can help engineers to have qualitative insights into, for example, the shoreline evolution in response to a new coastal structure, or to face with management strategies, when involving beach nourishment projects.

The bypassing conditions **Eq. (3a-b)** are essential to understand the limits of the approach. Fundamentally, they hypothesize that the bounding outcrops are long enough to prevent any littoral transport at the very initial instants of the evolution; then, the sand flow increases linearly with y until the structure's head is reached ($y = l_{h1,2}$) and the original shoreline potential flow rate is restored ($\partial y / \partial x = 0$). Accordingly, if the bounding outcrops are too short, and a **significant bypass occurs at the earlier stages of evolution**, the theoretical solution may strongly diverge from the real evolution process.

This would narrow the scope of Eqs (4) and (5) to newly designed structures, excluding, e.g. saturated groin compartments, affected by high bypass rate. This aspect is deepened in the following **section**.

2.1. Closed VS semi-bypassed groin compartment

For both an insulated beach ($l_{h,1} = l_{h,2} \to \infty$) and a stretch of coast bypassed at one end ($l_{h,1} \neq 0;\ l_{h,2} \to \infty$), the solution of the Neumann problem is trivial, and the Robin system gives the whole beach planform evolution.

In the case of infinitely long outcrops, we have:

$$y^{'}(x,t) = \sum_{n=0}^{\infty} y_n^{'} \cos\left(\frac{n\pi}{L}x\right) e^{-\varepsilon \mu_n{}^2 t} \tag{6}$$

in which the coefficients $y_n^{'}$ are calculated by the initial condition $y^{'}(x, 0) = g^{'}(x)$.

$$y_n^{'} = \frac{2}{L}\int_0^L g^{'}(x) \bullet \cos\left(\frac{n\pi}{L}x\right) dx \tag{7}$$

Eq. (6) matches with the solution by Hoang (2020) if the wave angle equals zero.

On the other hand, for a semi-bypassed compartment one has:

$$y^{'}(x,t) = \sum_{n=0}^{\infty} c_n \cos[\mu_n (x - L)] e^{-\varepsilon \mu_n{}^2 t} \tag{8}$$

where:

$$c_n = \frac{2}{L}\int_0^L g^{'}(x) \bullet \cos[\mu_n (x - L)] dx \tag{9}$$

The coefficient μ_n are the modes of the relationship:

$$\tan(\mu_n L) = \frac{\mu_n \bullet \left(\frac{|\theta_b|}{l_{h,1}} + \frac{|\theta_b|}{l_{h,2}}\right)}{\mu_n^2 - \frac{\theta_b^2}{(l_{h,1} \bullet l_{h,2})}} = \frac{1}{\mu_n} \frac{|\theta_b|}{l_{h,1}} \tag{10}$$

2.1.1. Validity of the semi-bypassed solution

A fundamental assumption of our approach is that a theoretical solution may be applied even beyond the strict hypotheses of DSE (e.g. small wave angle), as long as it exhibits a reasonable agreement with the numerical solution of OLCE; the latter is in principle more general than the diffusion equation and tends towards it for small obliquity. To this end, we use the software GENESIS (Hanson and Kraus, 1989) as a benchmark, because of its wide validation against real cases of shoreline evolution.

Eqs. 8–10 have in fact two limitations, **above that related to the DSE itself**, one related to the wave angle and the other related to the length of the bypassed outcrop. Ciccaglione et al. (2023) studied the effect of wave obliquity and observed that the agreement between numerical and analytical outcomes was reasonable up to an offshore wave angle of 35° relative to the shoreline orientation (maximum difference less than 30%, Fig. 2). This is indeed surprising given the rather simplified representation of the bypass process in Eqs, (3).

In this article, 50 new numerical experiments were carried out to investigate the influence of the bypassed groin's length. Unlike the effect of the wave angle, it should be noted that the results presented below are inherently empirical, as in GENESIS the effect of bypass is treated pragmatically (Buccino et al., 2020a, b, c) and does not rely on firm theoretical basis.

The tests consist of a 100 m wide rectangular beach nourishment in a 1 km compartment as shown in Fig. 3a. The compartment is bounded by an infinitely long jetty at the right end, while the length of the left closure was varied between 10 m and 200 m. The beach is made of medium sand ($d_{50} = 0.4$ mm), and has a depth of closure (Hallermeier, 1981) of 7 m, 220 m far from the initial shoreline (Bruun, 1954; Dean, 1977). The offshore wave angle was varied between 0° and 30°, while the wave height and period were set on 0.8 m and 6s, typical values of the most frequent waves in the Mediterranean Sea.

It was noticed that for very short groins at the left end, the shoreline retreats yet at the earliest evolution time steps; analytical and numerical solutions diverge in the neighbourhood of the bypassed outcrop, as indicated by the red dot curve in Fig. 3b. The "nonconsistency area" then progressively enlarges in time, extending towards the right end (blue dot line in Fig. 3b). The general characteristics of the evolution were found to be independent of the wave angle.

To establish a reliability domain, Fig. 4 plots the analytical to numerical shoreline position ratio, after one year simulation time, at x = 0. The abscissa reports the theoretical share of bypass:

$$R_{BYP\%} = (1 - L_G / L_{D_c}) \bullet 100 \tag{11}$$

in which L_G denotes the bypassed groin length and L_{D_c} is the distance of the closure depth to the initial shoreline.

The results indicate a conventional reliability border at $R_{BYP\%} \approx 85\%$, (red dashed line of Fig. 4), after which the analytical to numerical ratio starts to continuously decrease. Noteworthily, negative values are attained by small wave angles first, since the loss due to bypass is not compensated by the littoral drift in the central part of the coast.

It should be highlighted that previous outcomes are independent of the transport coefficient K_1 in GENESIS, as the diffusivity coefficient in Eq. (1) has been adjusted for each experiment to follow the evolution of the numerical beach. More details can be found in Ciccaglione et al. (2023).

2.2. Analytical solutions and engineering applications

For practical purposes, finite beach solutions of DSE can be profitably used to analyse the mid to long term evolution of a beach nourishment project.

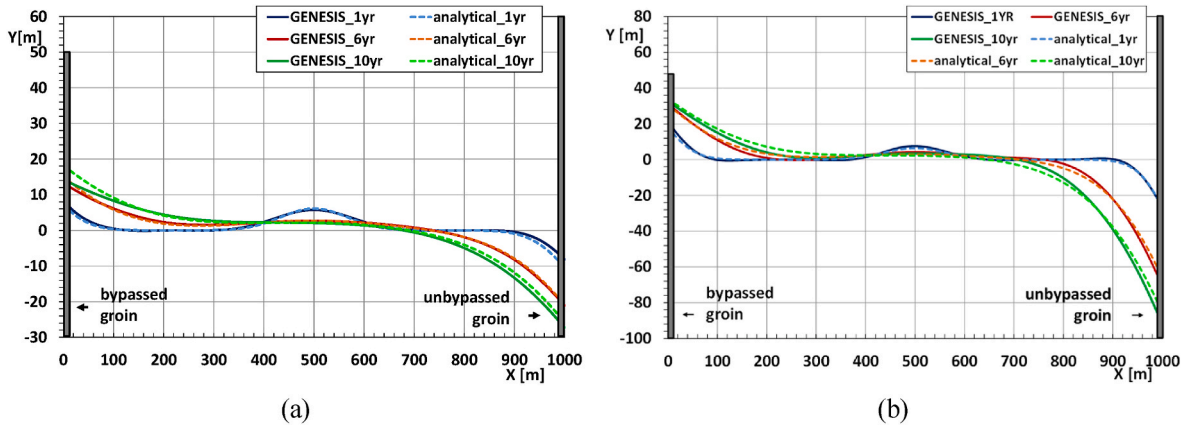

Fig. 2. (a) Comparison between analytical and numerical shoreline position for 5° of offshore wave angle; (b) Comparison between analytical and numerical shoreline position for 35° of offshore wave angle. It is seen the progressive mismatch at the domain bounds (Ciccaglione et al., 2023).

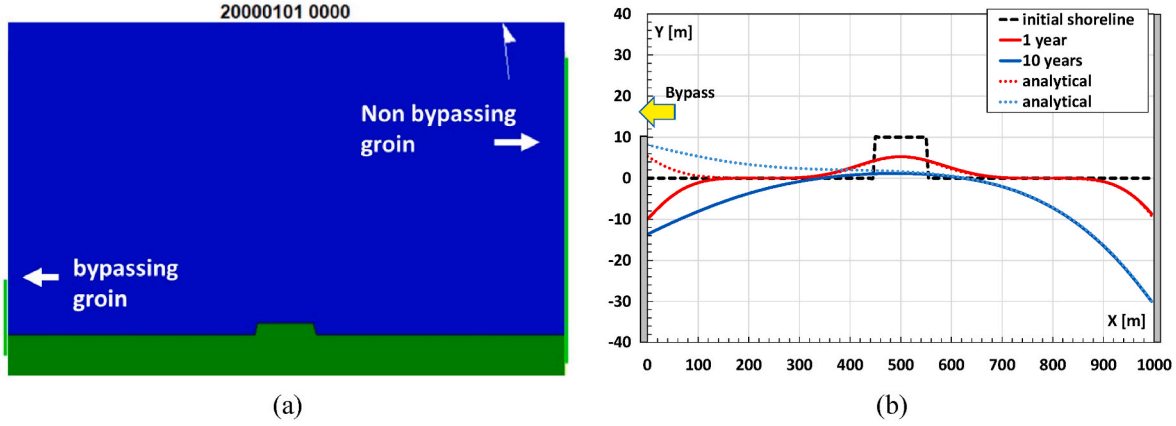

Fig. 3. Panel (a). GENESIS modelling of the 1 km long bypassing compartment. Panel (b) Comparison between analytical and numerical solution for a short (bypassed) 10 m groin. Red solid/dot lines, 1 year of evolution; Blue solid/dot lines; 10 year of evolution.

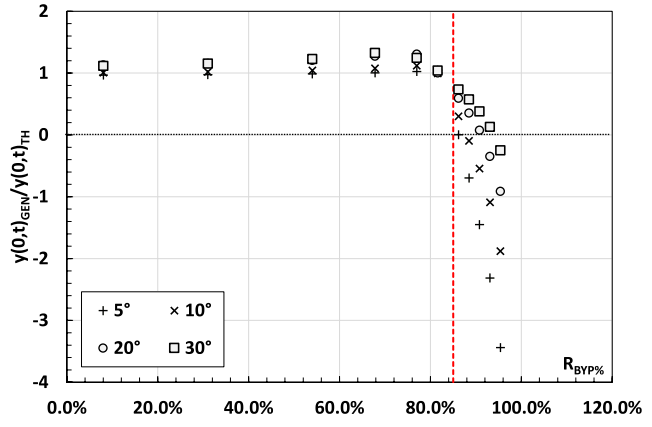

Fig. 4. Reliability domain of Eq. (8) regarding the shortness of the bypassed groin.

As is known, a ruling variable for management is the time interval t_M needed to reduce the initial fill volume to a certain percentage M. t_M solves the equation:

$$M = \frac{V(t_M)}{V_0} = \frac{\int_{x_0}^{x_1} y(x, t_M)dx}{\int_{x_0}^{x_1} y(x, 0)dx} \tag{12}$$

in which x_0 and x_1 are the extremes of the project. Above all, two percentiles can be of significance for engineering purposes, namely the "half-life" and "quarter-life" reduction times, t_{50} and t_{25}. They represent the status where the design conditions are no longer met, and namely the Serviceability Limit State (SLS) and the Ultimate Limit State (SLS), respectively.

For a rectangular beach fill of width B placed symmetrically within an insulated beach of length L, Ciccaglione et al. (2023) found:

$$t^*_{M,ins} = \max\left(0.0206\, M(t)^{-4.244}; 78.213\, \exp(-7.047 M(t))\right)\left(\frac{B}{L}\right)^2 \tag{13}$$

in which the characteristic times are made nondimensional according to:

$$t_M{}^* = \varepsilon\left(\frac{n\pi}{L}\right)^2 t_M \tag{14}$$

where ε is the shoreline diffusivity. The calculation of the diffusivity parameter has been extensively discussed in both Ciccaglione et al. (2023).

In a semi bypassed compartment, a lower lifetime is expected. The reduction will be the more significant the larger the width of the project, as the bound of the nourishment approaches the bypassed groin, and the more oblique are the waves. This is shown in Fig. 5, which compares the reduction curves $M(t^*)$ of two nourishments with $B/L = 0.1$ (Panel a) and $B/L = 0.3$ (Panel b).

Clearly, the rate of bypass, $R_{BYP\%}$, will also affect the solution. After extensive curve fitting (Fig. 6), the following polynomial form can be

proposed:

$$\sqrt{\frac{t_{M,ins}}{t_{M,byp}}} = \boldsymbol{a}\left[\left(\frac{B}{L}\right)^2 \bullet \alpha^{0.2}\right]^2 + \boldsymbol{b}\left[\left(\frac{B}{L}\right)^2 \bullet \alpha^{0.2}\right] + \mathbf{1} \tag{15}$$

where α is the wave angle (in radians) and coefficients $\boldsymbol{a}$ and $\boldsymbol{b}$ vary with the bypass ratio. Values for $M = 25$ and $M = 50$ are reported in Table 1.

The inspection of Equation (15) and Table 1 reveals the following point of interest:

a) for a normal wave attack, $\alpha = 0$, the bypassed groin has obviously no influence as no littoral drift takes place;
b) the lifetime ratio is more sensitive to the project width than the wave angle;
c) the bypass boundary condition has practically no effect on t_{50} as B/L is less than approximately 0.25. The limit drops to 0.1 for t_{25}. In both cases using Eq. (13) leads to an error not larger than 5%.

On a more general level, the fact that a bypassing compartment reduce the expected project lifetime should lead engineers towards conceived management strategies for the periodic refill of the nourishment. To aid this process, we note that Eq. (15) expresses anything but the amplification of the nourishment refill (ARF) due to bypass. Therefore, it can be of interest to assess the conditions for which the refill time is magnified by a factor of 1.25, 1.5, 2 and 3, which is reported in terms of the variable $\left(\frac{B}{L}\right)^2 \bullet \alpha^{0.2}$ in Table 2 for application purposes.

The same concept is shown in a graphical form in Fig. 7.

It is finally recalled that previous results hold for a rectangular beach fill placed symmetrically in a bypassed cell and are strictly limited for $0 < \left(\frac{B}{L}\right)^2 \bullet \alpha^{0.2} < 0.1859$ and $0 < \left(\frac{B}{L}\right)^2 \bullet \alpha^{0.2} < 0.05$, for the "half-life" and "quarter-life" reduction times, respectively.

3. Bounded domain with highly bypassing groin

Fig. 4 of section 2.1.1. clearly limits the theoretical solution to "not too short groins". A limited length of the bypassed outcrop produces, in fact, a significant sand bypass at the earlier stages of the evolution and, consequently, a fast updrift retreat of the shoreline.

From a physical point of view, the solution fails to account for a convection process which adds to the diffusion one. As such, a more rigorous path might be the resolution of the Advection-Diffusion equation, as indicated by (Huisman et al., 2013); alternatively, one can roughly fix the problem adding some "convective terms" to the diffusive solution. **That's exactly why the cases presented in the following sections appear to be physically unusual, since the bypassing rate seems to exceed the longshore transport rate.**

Nevertheless, the latter approach proves to be surprisingly efficient (Section 3.1), so that it is further applied to model the effect of a compartment in which a certain amount of sand is entering the domain from the outside.

3.1. Approximate solution for exiting bypass

A non-rigorous but physically consistent solution to the "early bypass" problem is achieved by adding Eq. (8) with a fictional transport source concentrated at x = 0. The latter, say $y_{BYP}(x,t)$, is modelled via the truncated response of an unbounded domain to a negative Heaviside step function:

$$y_{BYP}(x,0) = K \bullet [H(x) - 1] \tag{16}$$

DSE solution to the initial profile of Eq. (16) in the interval $(0, L)$ eventually yields (Fig. 8):

$$y_{BYP}(x,t) = -\frac{K}{2} \bullet erfc(x^*) \bullet Rect\left(x - \frac{L}{2}\right) \tag{17}$$

with:

$$x^* = \frac{\pi}{2} \bullet \frac{x}{L} \bullet \frac{1}{\sqrt{t^*}} \tag{18}$$

The scale parameter K has to be adjusted to match the volume of sand, V_{BYP}, that bypasses the domain over a given time interval, t^*. This results in the following balance equation:

$$\int_0^L y_{BYP}(x,t)\,dx = \frac{\exp(-x^{*2}) \bullet (\sqrt{\pi} \bullet (x^* \exp(x^{*2}) \bullet erf(x^*) - x^* \exp(x^{*2})) + 1)}{\pi\sqrt{\pi}\,(0.8\,K \bullet L \bullet \sqrt{t^*})^{-1}} = \frac{V_{BYP}}{(h_c + B)} \tag{19}$$

which is solved for K.

The approach is not expected to hold as $t^* \to 0$, since the sand transport **would increase indefinitely**. The comparison with GENESIS

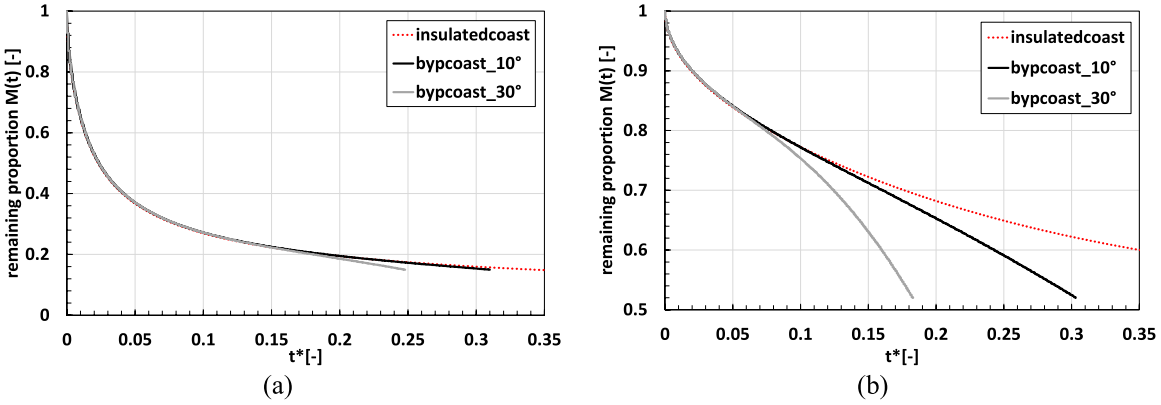

Fig. 5. Proportion of sand remaining at the placement site of the rectangular nourishment for the bypassed compartment and comparison to the insulated curve (red dot line). Panel (a) B/L = 0.1; Panel (b) B/L = 0.3.

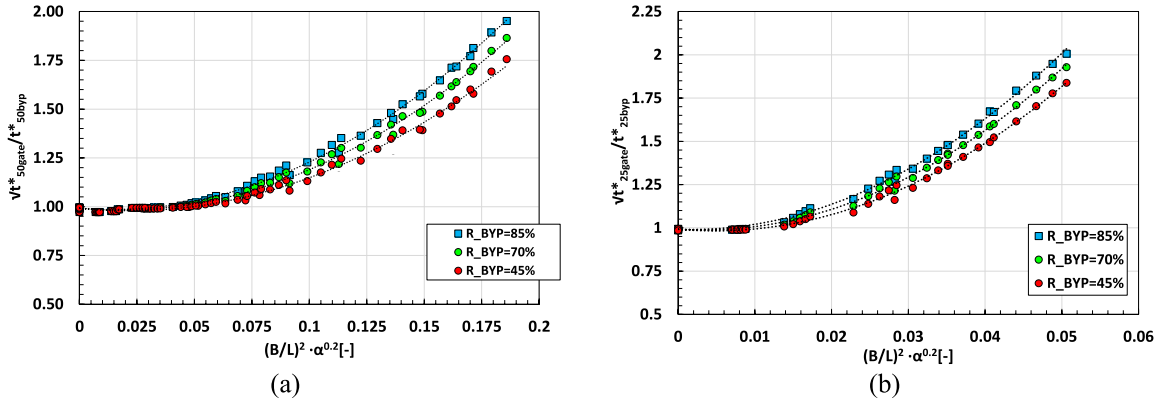

Fig. 6. Curve fitting analysis for the insulated/bypassed compartment as a function of the beach nourishment width and the wave angle. The black dot lines indicate Eq. (15). Panel (a) $\sqrt{t^*_{50gate}/t^*_{50byp}}$. Panel (b) $\sqrt{t^*_{25gate}/t^*_{25byp}}$.

Table 1
Coefficient of Eq. (15) for M = 50 and M = 25 for different bypass rates.

$R_{BYP\%}$	a (t^*_{50})	b (t^*_{50})	R^2 (t^*_{50})	a (t^*_{25})	b (t^*_{25})	R^2 (t^*_{25})
86%	32.904	−0.9234	0.9975	437.36	−1.5319	0.9974
72%	30.714	−1.0955	0.9962	426.61	−2.7734	0.9973
60%	29.390	−1.1179	0.995	418.88	−3.1839	0.997
45%	27.542	−1.1925	0.9932	408.74	−3.9371	0.9966

Table 2
Range of influence of the Amplification Refill Factor for M = 50 and M = 25.

Amplification Refill Factor (ARF) $t^*_{M,ins}/t^*_{Mbyp}$	R_{BYP} %	$(B/L)^2*\alpha^{0.2}$ [t^*_{50}]	$(B/L)^2*\alpha^{0.2}$ [t^*_{25}]
3	86%	0.1647	0.043
	72%	0.1741	0.045
	60%	0.1789	0.046
	45%	0.187	0.048
2	86%	0.1282	0.033
	72%	0.1359	0.035
	60%	0.1404	0.036
	45%	0.1467	0.037
1.5	86%	0.0994	0.025
	72%	0.1067	0.027
	60%	0.1101	0.028
	45%	0.1161	0.029
1.25	86%	0.0775	0.019
	72%	0.0843	0.021
	60%	0.0875	0.022
	45%	0.0929	0.023

resulted in a remarkable agreement for a wide spectrum of shoreline shapes and wave angle. As an example, Fig. 9 shows the cases of compartments of different widths, with or without a beach fill profile. The numerical analysis indicated a satisfactory agreement even for t^* of the order 0.01.

It is of interest to remark that for very short stretches of coast, where t^* is large, Eq. (16) evolves soon towards the equilibrium, and the bypassing effect reduces to a mere backward translation of the equilibrium shoreline, as $y_{BYP}(x,t) \rightarrow -K/2$ (solid grey line in Fig. 8).

3.2. Application for entering bypass

The approach of the "concentrated transport" is further applied to model the case of a beach compartment fed from the outside. Intuitively, this condition matches the analytical solution for an insulated beach, Eq. (6), as long as the bypassing rate is low (that is, the bypassed groin in Fig. 10a is sufficiently long). By contrast, as the bypassing rate enhances, the insulated beach solution fits properly only the shoreline position at the downdrift end (Fig. 10b), while at the updrift side the feeding volume mitigates the erosional area.

Therefore, to account for the entering volume, a term is added which corresponds to a positive Heavyside step, concentrated at $X = L$. The correction shoreline function is then:

$$y_{BYP}(x,t) = +\frac{K}{2} \bullet erfc(x^*) \bullet Rect\left(x - \frac{L}{2}\right) \tag{20}$$

in which K is still ruled by the mass balance of Eq. (19).

As for Section 3.1, the use of Eq. (14) resulted in a fair agreement between theoretical and numerical shoreline planforms. An example is given in Fig. 11, which compares the solutions for different values of the dimensionless time parameter t^*. As the nondimensional time is small (Panel a), the effect of the concentrated transport is reducing the erosion area at the updrift side. On the other hand, as the time increases and the diffusion process is almost exhausted, the Heavyside function leads approximately to a translation of the planform, as in Panel b.

The good agreement in the numerical simulations has suggested an application to a real-life case, which is discussed below.

3.3. Application to the Emilia Romagna case of study

The concepts above discussed are employed to analyse the response of a stretch of coast located in the southern part of the Romagna riviera. It extends for about 11 km, from the Rimini port to the north to the Riccione port to the south and fronts the Adriatic Sea with an average orientation of 40°N (Fig. 12).

The port structures form a groin cell, which is included in the wider physiographic unit of Rimini-Cattolica, of about 20 km long (Fig. 12). The sediment sources which contributed to the natural nourishment of the coastal stretch include the Marche coastline, particularly the Gabicce promontory, and the Conca River in the southern section. This produced a uniform grain size distribution across the beaches, as confirmed by the extensive sediment campaign carried out by the Emilia Romagna Region in 2012. Sediment samples taken to a depth of 7 m primarily consist of fine sand (d_{50} = 0.2 mm) throughout all depths, with sorting varying from moderate to poor in deeper seabed. The samples predominantly exhibit negative asymmetry on the emerged beach and positive asymmetry on the submerged one.

Starting from the second half of the last century, the Rimini-Cattolica coastal system has undergone deep anthropogenic transformations, leading to the disappearance of much of its original landscape and environmental characteristics, along with a reduction in the areas affected by natural coastal processes. The construction of ports, river basin regulation, and channel excavation have resulted in the loss of sediment supply to the coastlines. Additionally, the extraction of fluids

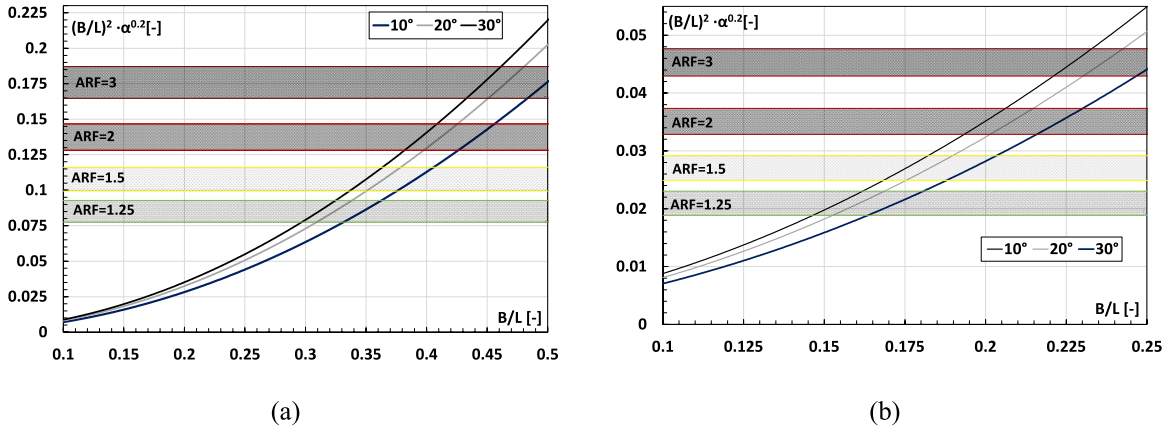

Fig. 7. Range of influence of the Amplification Refill Factor for M = 50 and M = 25 in graphical form. Curves are differenced with respect to the wave angle.

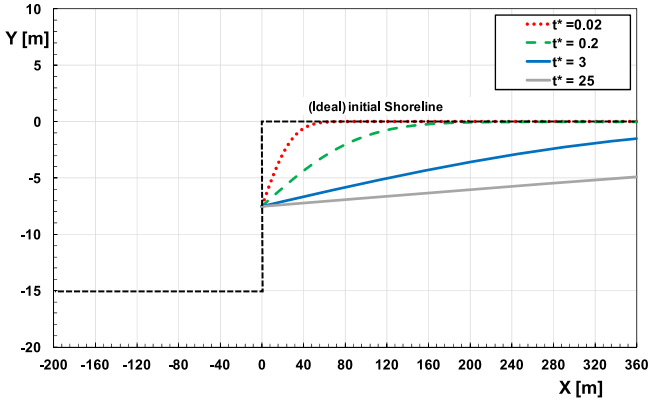

Fig. 8. Approximate bypass correction, $\mathbf{y}_{BYP}(\mathbf{x}, \mathbf{t})$, for different t*.

(water and gas) from underground sources has increased the subsidence rate, resulting in a loss of beach volume. Furthermore, the urbanized surface area along the coast has expanded significantly, with a 500% increase over the past 60 years within approximately 1.5 km from the shoreline.

Consequently, the sandy coast has undergone a remarkable mid-term retreat process. Particularly, the shoreline progressively advanced at the Rimini jetty (**built in 1933**), while significant erosion occurred to the south of Riccione port (**built in 1943**) **up to Cattolica port**, suggesting the presence of a littoral transport moving from south to north.

Over the years, numerous interventions have been carried out (or designed) to address the issue of erosion, aiming to locally mitigate coastal erosion processes and protect residential areas. This also includes environmentally friendly solutions, such as Reef-Balls™ (Buccino et al., 2013) and Wmesh (www.edilimpianti.it), which are intended to favour the interaction with mine flora and fauna. In fact, the southern part of the Rimini-Cattolica coastal segment have been deeply modified by the construction of numerous hard protection structures, both detached (emerged and submerged) breakwaters, and groins. The rigid approach, initially performed by the local administrations, has been progressively shifted toward nature-based solutions and coastal management strategies (e.g. artificial nourishments), to minimize environmental impacts. However, those strategies involved prevalently the southern part of the unit, while the Rimini-Riccione beach cell, that under study, remained non structured over years, given its accretive trend.

As such, Rimini jetty is to reach the closure depth (about 7 m), **thus**, totally blocking longshore transport, while Riccione jetty extends toward 1 m depth, weakly acting on the sediment flow; therefore, a significant bypass occurs at the Riccione location, as corroborated by the frequent and significant siltation of the port mouth (Arpae, 2016). Fig. 13 gives an insight, plotting the evolution of the compartment given the shorelines surveys from 1955 to 2016 (Arpae, 2016; CUGRI - Consorzio inter-Universitario per la previsione e prevenzione dei GRandi rIschi, 2018). **Minor variations in beach profile are noted, attributed to the relative stability of a bow-shaped beach positioned between the walls of two ports.**

Being part of the central Adriatic Sea riviera, Romagna coast is

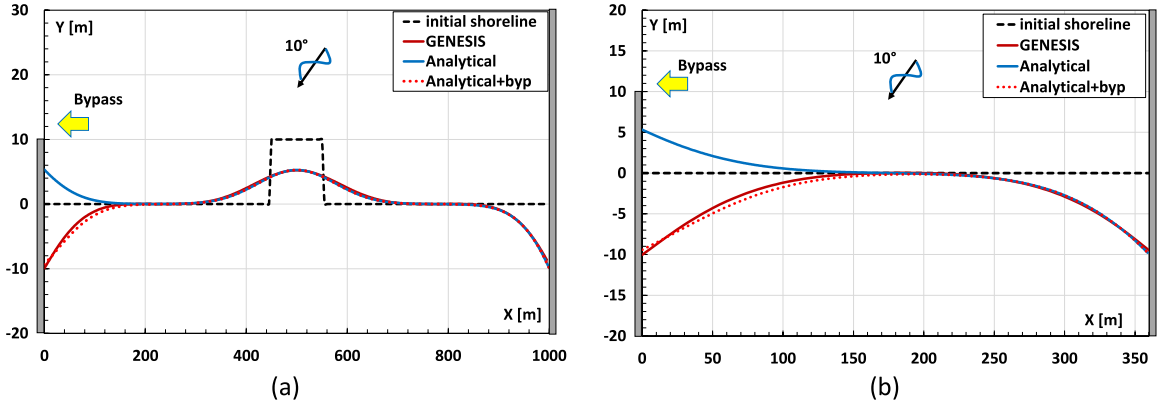

Fig. 9. Comparison between analytical and numerical solution after adding the approximate solution y_{BYP}. Left panel: 1000 m domain for t* = 0.0244. Right panel: 360 m domain for t* = 0.1889.

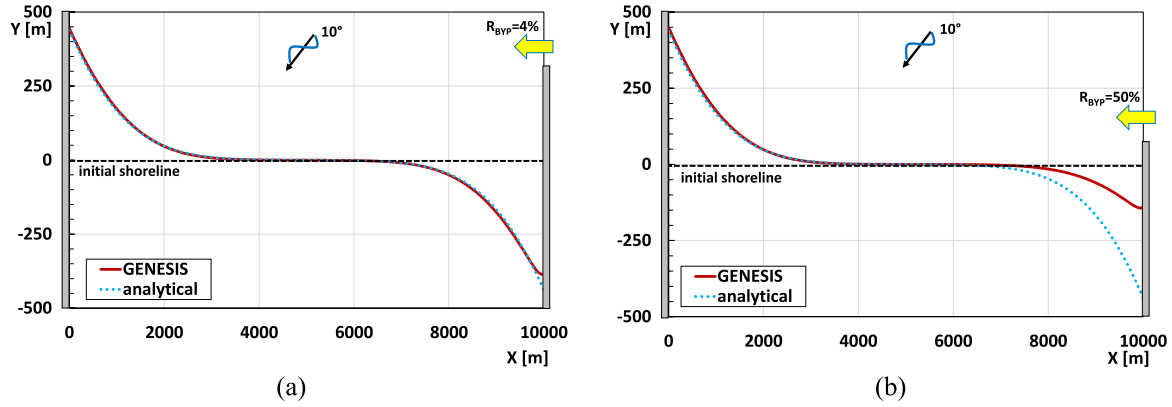

Fig. 10. Comparison between Eq. (6) and numerical solution for a bypassing groin compartment. Panel (a) bypass rate 4%. Panel (b) bypass rate 50%.

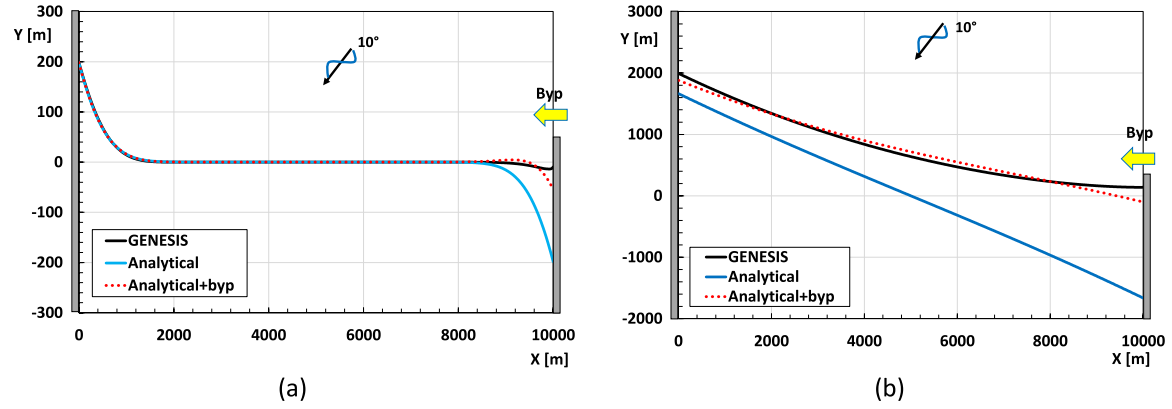

Fig. 11. Comparison between Eq. (6) and numerical solution after adding the approximate solution y_{BYP}. Panel (a) $t^* = 0.0224$. Panel (b) $t^* = 2.44$.

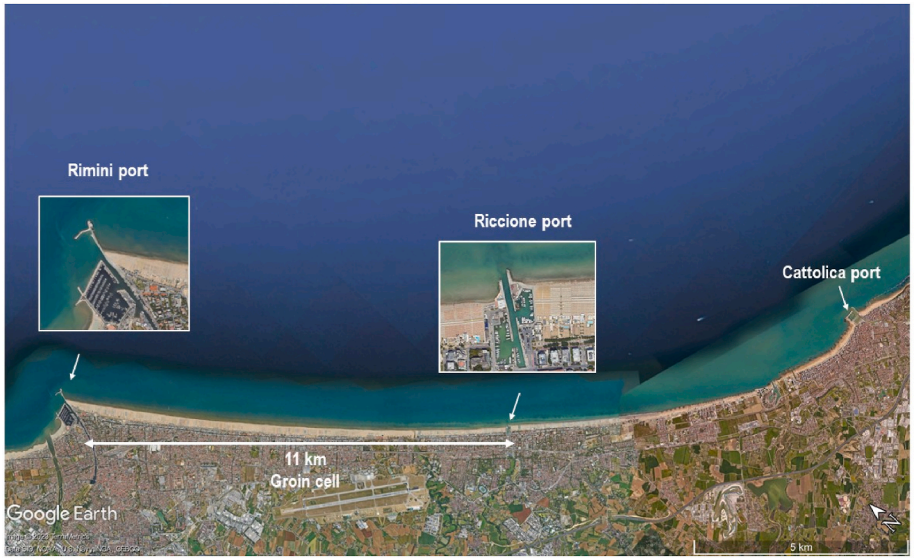

Fig. 12. The sand beach compartment between Rimini port and Riccione port, included in the wider physiographic unit of Rimini-Cattolica. The smallest panels give an insight on the port's jetties.

featured with a wide wave compass, virtually covering an arch of directions ranging from 310°N to 130°N. Wave climate analysis has been performed by considering data registered by Cesenatico wave buoy, located 8 km offshore from the coast, at a depth of about 10 m, practically in the nearshore zone (CUGRI - Consorzio inter-Universitario per la previsione e prevenzione dei GRandi rIschi, 2018). Fig. 14 **(Panel a)** shows how climate is featured with a single mode with predominant wave attacks coming from east quadrant, around 100°N. Moreover, the physiographic unit is characterized by a yearly depth of closure D_c of about 7 m (Hallermeier, 1981), while an average berm height B of 1 m

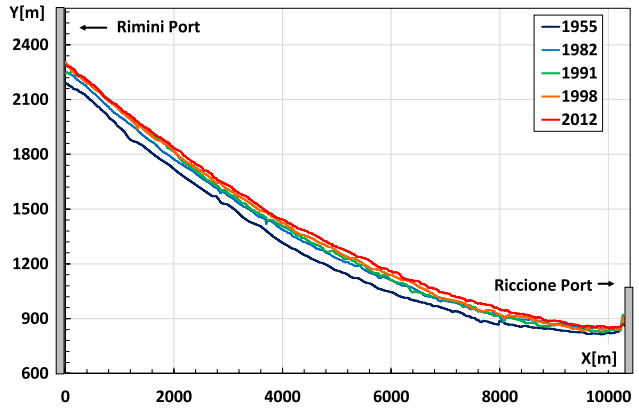

Fig. 13. Evolution of the groin compartment between Rimini and Riccione ports from the shorelines surveys from 1955 to 2016 carried out by Arpae Emilia-Romagna, 2016.

was estimated, based on profile surveys (CUGRI report).

Littoral drift characteristics are graphically represented in Fig. 14 (Panel b) via the Littoral Drift Rose (LDR), which gives the potential littoral transport, Q, as a function of shoreline orientation β (Walton and Dean, 1973, 2010). LDR is based on the CERC formula for littoral drift (Shore Protection Manual SPM, 1984), giving:

$$Q(\beta) = \sum_{\alpha_{0i}=\beta-\pi/2}^{\alpha_{0i}=\beta+\pi/2} p_i \bullet \frac{K \bullet \left(H_{s0,i}\right)^{2.4} \bullet \left(T_{p0,i}\right)^{0.2} \bullet g^{0.6}}{16 \bullet (s-1) \bullet (1-n) \bullet \pi^{0.2} \bullet \gamma^{0.4} \bullet 2^{1.4}} \; sin[2(\beta - \alpha_{0i})] \tag{21}$$

where:

- g is gravity;
- $s \approx 2.6$ is the ratio between the specific gravity of sediment and that of water;
- $n \approx 0.4$ is the in place porosity;
- $\gamma \approx 0.6$ is the breaker index (wave height to depth ratio, **Kamphuis, 1991**);
- H_{s0} denotes offshore significant wave height;
- T_{p0} is the peak period;
- α_0 is the azimuth from which waves originate.

From the LDR graph the littoral transport is nullified at an orientation of 60°N; therefore, the entire diagram can be approximated by a single equivalent wave component, coming from 60°N and with $H_{m0,eq} = 0.8$ m and $T_{p,eq} = 5$s (broken line lobes of Fig. 14b).

Given that the coast is oriented toward 40°N on average, **the equivalent wave is seen to produce** a significant littoral transport that moves sediments from south to north, **this is so that it is in fair agreement with the observation of the general trend of the coast**.

A transport coefficient K of the order of magnitude of 0.1 has been calibrated to obtain a fair consistency with the volumetric analysis performed by Arpae Emilia-Romagna between 2006 and 2012 (Arpae, 2016; CUGRI - Consorzio inter-Universitario per la previsione e prevenzione dei GRandi rIschi, 2018), which is reported in the following Section. **(See Appendix 1 for a detailed description of the K calibration).**

3.3.1. *The estimation of the longshore transport rate from the volumetric analysis of the Arpae (2016)*

A fairly accurate volumetric analysis concerning the main physiographic unit between the ports of Cattolica and Rimini was carried out by Arpa Emilia Romagna in the period 2006–2012. The study reports the volume variation experienced by limited sections of the coast, the volumetric losses due to subsidence, the nourishment volumes and any other artificial removal.

A critical limit of the analysis, **which consequences are discussed in this section**, **consists in** a control volume that extends from the shoreline up to a depth of 2.5 m; this volume is therefore only a portion of the active beach profile, since the seasonal closure depth has been estimated at 7 m.

The mass conservation has been applied to the entire coast between Rimini and Cattolica:

$$\frac{\partial A}{\partial t} + \frac{\partial Q_l}{\partial x} = q_{in} - q_{out} \tag{22}$$

where, A is the cross-sectional area of the beach between the active berm and the closure depth (m^3/m), Q_l is the littoral drift (m^3/year), q_{in} and q_{out} represent cross-shore inputs and outputs (e.g. canyons, artificial nourishment, subsidence, etc. in m^3/year m).

Firstly, Eq. (22) is applied to the entire physiographic unit, by spatially integrating between Cattolica (x_C abscissa) and Rimini (x_R abscissa), yelding:

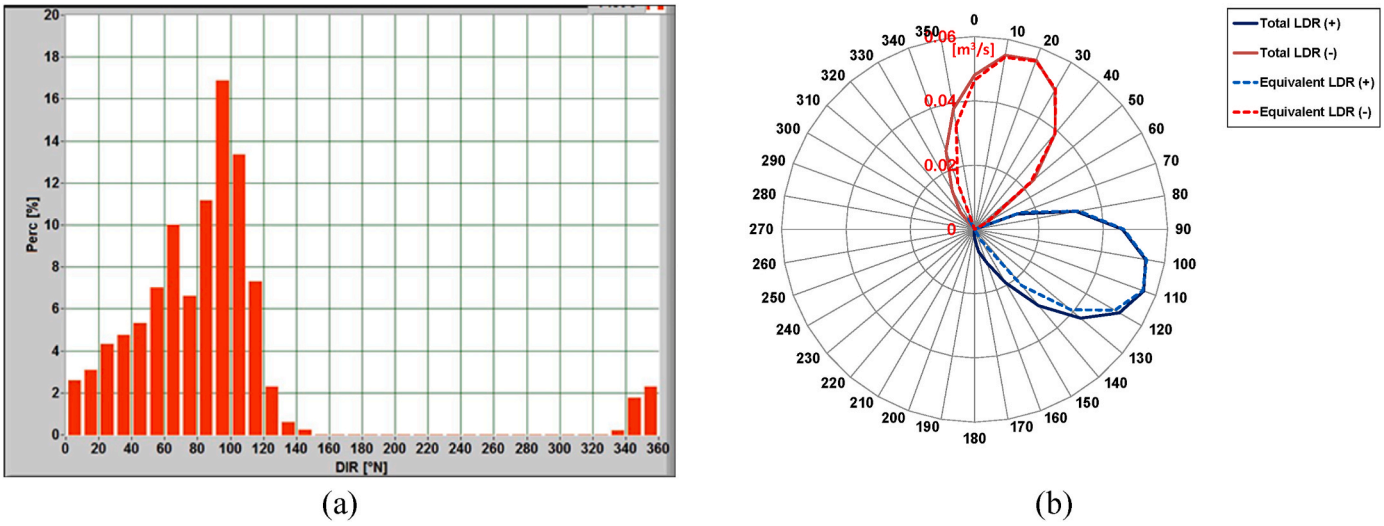

Fig. 14. Panel (a). Annual Histogram of wave directions for angular sector of 10° for the Emilia Romagna coast. Panel (b). net littoral drift rose of Emilia Romagna coast; blue solid line represents drift to right when looking offshore, while red solid line represents drift to left when looking offshore. Dotted lobes give the Equivalent LDR. Littoral drift in cubic meters per year.

$$\frac{\partial}{\partial t}\int_{x_R}^{x_C} A\,dx + Q_l(x=x_C) - Q_l(x=x_R) = \int_{x_R}^{x_C}(q_{in} - q_{out})dx \tag{23}$$

In which the alongshore abscissa was assumed to be oriented from Rimini toward Cattolica. Since the stretch considered is a physiographic unit, it follows that $Q_l(x = x_C) = Q_l(x = x_R)$, for which Eq. (23) is reduced into:

$$\frac{\partial}{\partial t}\int_{x_R}^{x_C} A\,dx = \int_{x_R}^{x_C}(q_{in} - q_{out})dx \tag{24}$$

Which equals the total volume change to the difference between the cross-shore inputs and losses. Therefore, by denoting first member as V_{beach}, and by integrating with respect to time we obtain:

$$\Delta V = (V_{beach})_{t_{fin}} - (V_{beach})_{t_{in}} = V_{in} - V_{out} \tag{25}$$

where V_{in} and V_{out} represent source and sink volumes in the considered time interval.

The Arpae detects a negative volume variation $\Delta V = -423'529\ m^3$ in the 6 years, between 2006 and 2012. In the same period there was an input for artificial nourishment of $641'009\ m^3$, a material withdrawal of $162'234\ m^3$ and a loss due to subsidence of $110'892\ m^3$ (see also Table 3). It is evident that the inputs exceed the losses: $\mathbf{641'009 m^3 - 162'234 m^3 - 110'892 m^3 = 367'883 m^3}$ and to close the sediment balance an additional loss, V_{sto}, has been considered:

$$\mathbf{-423'529 m^3 = 367'883 m^3 - V_{sto} \quad \rightarrow \quad V_{sto} = 367'833 m^3 + 423'529 m^3 = 791'412 m^3} \tag{26}$$

The loss in Eq. (26), has been realistically related to storms, which move sediment toward the depth of closure to form the winter bar. The no-balance in the sediment budget likely arises from the volumetric surveys conducted by ARPAE, which only reach depths of up to 2.5 m and do not encompass the seasonal closure depth, beyond which sediment transport is deemed negligible. Hence, it is reasonable to posit that the deficit highlighted by Eq. (26) stems from sediment discharge beyond the 2.5-m depth, triggered by cross-shore transport during storms. This deficit is subsequently incorporated back into the sediment budget to achieve equilibrium.

The volumetric loss due to storms is assumed to be uniformly distributed along the physiographic unit, which extends from Rimini to Cattolica, covering a length of 19′390 m. With an observation period of 6 years, the resulting discharge per unit length is $q_{sto} = 6.80\ m^3$/year m.

Therefore, Eq. (22) can be applied to the stretch of coast between Rimini and the last detached breakwater of Misano Adriatica, which is a subset of the broader physiographic unit of Rimini-Cattolica (Fig. 15). Moreover, the Misano breakwater is supposed to block the longshore sediment transport. Eq. (22) is, then, formulated as follows:

$$\frac{\Delta V_{stretch}}{6\ years} + Q_l(x+\Delta x) - Q_l(x) = \frac{V_{nour}}{6\ years} - \frac{V_{withdraw}}{6\ years} - \frac{V_{subsid}}{6\ years} - q_{sto}\Delta x \tag{27}$$

where Δx represents the length of a single stretch of coast.

Table 3 reports results for every coastal segment, while Fig. 16 littoral drift for the entire Rimini-Misano unit.

The graph shows a negative littoral drift directed from south to north, in line with the general observations. The Q_l gradient is negative in the section that goes from Rimini to the port of Riccione (x = 11000 m), indicating a potentially accretive trend of this stretch of coast. Moreover, at the Riccione port location, Q_l attains its maximum, equal to 45282 $m^3/year$, and grows rapidly southwards, suggesting a structural erosive trend.

3.3.2. Application of the analytical approximation for bypass

Based on the equivalent wave parameters above mentioned, one can easily calculate the site diffusivity according to Walton and Dean (2010):

$$\varepsilon = \frac{K \bullet (H_{s0,eq})^{2.4} \bullet (T_{p0,eq})^{0.2} \bullet g^{0.6}}{8 \bullet (s-1) \bullet (1-n) \bullet \pi^{0.2} \bullet \gamma^{0.4} \bullet 2^{1.4}} \bullet \frac{1}{D_c + B} \bullet cos[2(40^\circ - 60^\circ)] = 946080\ m^2\ /\ year \tag{28}$$

which gives, **by applying Eq. (14) to the Rimini-Riccione stretch of coast**, a value of t^* for a single year of 0.05. Note that the t^* magnitude is not so large, given the wider domain considered; therefore, diffusion process coexists with advection process.

It is worth noticing that, in Eq. (28), the depth of closure D_c has been reduced, since the volumetric surveys carried out by Arpae Emilia-Romagna extended up to a depth **equal to** 2.5 m.

Nevertheless, the latter assumption is still tolerable. In fact, the breaking wave at 2.5 m equals 1.5 m, given a breaker index γ of 0.6. Within the Cesenatico wave climate, the probability of exceedance of this wave is 6%, which corresponds to 22 days in a year. Therefore, by reducing the area of the active beach profile, the significance of the littoral transport is fairly near to that of the closure depth.

From the volume analysis reported in the previous paragraph, it is seen that at the Riccione port location, a littoral drift of 45282 $m^3/year$ moves from south to north (Fig. 16), so entering the sandy cell between Riccione and Rimini port. Particularly, given the relatively small extension of the Riccione jetty, a bypass coefficient of $R_{BYP\%} = 80\%$ can be realistically set.

Fig. 17 compares the analytical solution, Eq. (6), and the positive heavy-side step solution of Eq. (20) added with the insulated beach solution with the general trend of the Romagna coast for the years 1982, 1991, 1998 and 2012.

It is seen that the solution for insulated coast alone (solid grey line in Fig. 17) is able to explain the general trend of the coast, but the shoreline position detected at the Riccione port is never achieved. By contrast, if the bypass approximation, Eq. (20), is added to the general solution, a better accordance is found out, which confirms the goodness of the solution.

4. Discussion

Analytical solutions, such as the Diffusion Shoreline Equation (DSE), offer a promising alternative to resource-intensive numerical simulations for managing coastal areas and projecting long-term shoreline evolution. However, while effective for open coast scenarios (Larson et al., 1987; Dean, 2003), analytical solutions encounter limitations in

Table 3
Characteristics of the stretch of coast involved in the volumetric analysis by Arpae and the calculated littoral drift Ql for each stretch of coast.

Stretches of coast		L[m]	ΔV[m^3]	V_{nour} [m^3]	V_{subsid}[m^3]	$V_{withdraw}$ [m^3]	Q_l[m^3/y]
Southward Riccione port	***Riccione sud***	1000	−539	279,750	3934	0	−39259.17
	Riccione Centro	1850	−80410	51,065	8208	0	−43241.42
	Riccione Alba Sud	840	−5867	9865	4757	0	−45282.25
Northward Riccione port	***Riccione Alba Nord***	1250	3181	0	5912	0	−38333.08
	Fogliano Marina	610	−5867	9865	4757	0	−32165.92
	Miramare	6190	−270,310	0	51,279	19,665	−26574.33
	Rimini Centro	1350	−64644	0	17,161	0	−21509.08

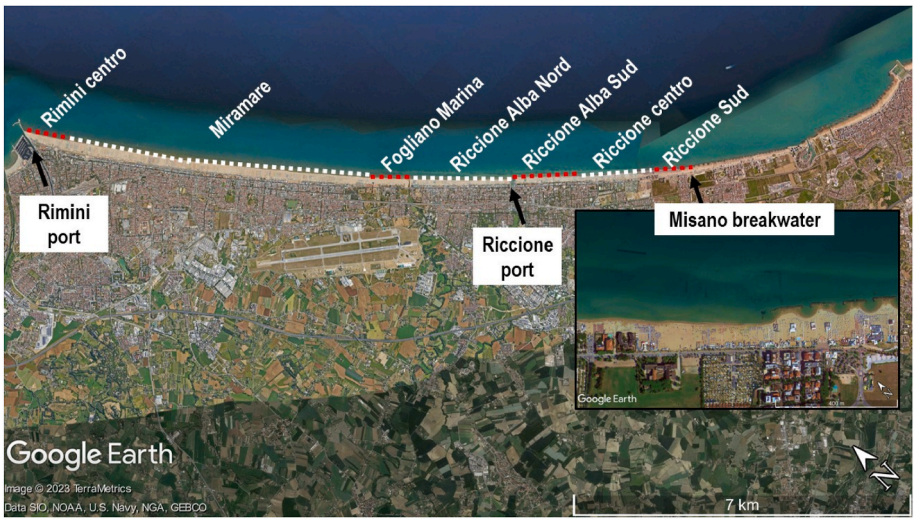

Fig. 15. Stretch of coast between Rimini and the last detached breakwater of Misano Adriatica, the red/white dotted lines indicate the sub segments for which the volumetric analysis by Arpae has been carried out.

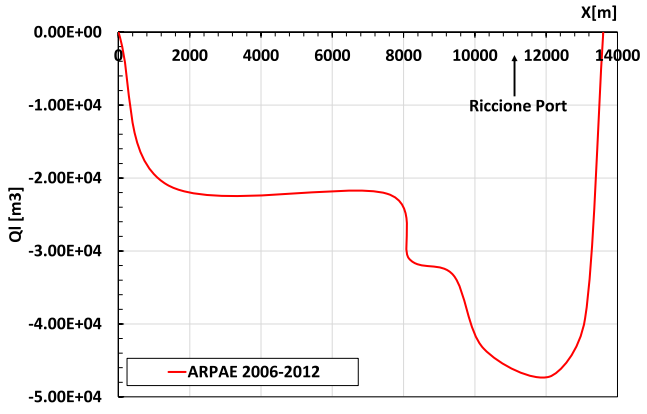

Fig. 16. Littoral drift for the entire Rimini-Misano unit determined from the volumetric analysis by Arpae.

closed domains (e.g. finite beaches bounded by varying lengths of outcrops). On the one hand, the remarkable works by Zacharioudaki and Reeve (2008) and Valsamidis and Reeve (2020) further enhanced knowledge on both single insulated groin compartment and groin field with bypass, respectively. However, a primary limitation of these studies lies in the complex mathematical forms, often comprising series of functions, which may restrict their practical applicability beyond the realm of advanced mathematics. On the other hand, Hoang (2020) formulated a concise solution for a beach bounded by groins of infinite length, but solely suitable for under wave attacks perpendicular to the shoreline.

In this regard, the work by Ciccaglione et al. (2023) tried to overcome these limitations by developing a general solution of the DSE, based on the sum of two Sturm-Liouville Boundary Value Problems (BVP), that apply to finite beaches bounded by outcrops of arbitrary length (including zero-length). The general form of the solutions allows to account for both bypassing and non-bypassing conditions, as well as wave obliquity.

Principally, main limitations of the analytical approach regard the assumptions of the diffusion equation itself, and namely small wave angle, mild shoreline gradient and stationary wave forcing. In this regard, the authors compared the analytical solutions to the numerical outcomes of the OLCE-based software GENESIS (Hanson and Kraus, 1989), to assess whether they could hold even beyond their theoretical limitation of small angle. Results confirmed that the solution can be reliably employed up to 30°. Therefore, a curve fitting study was carried out to turn the solutions into simple easy-to-use formulae of practical interest; this essentially concerned in the remaining value of sediments in a beach fill of rectangular shape for a finite beach either pinned by revetments at the extremes or bounded by unbypassed groins (insulated beach).

Starting from the previous results from Ciccaglione et al. (2023), this study aims at providing a further analysis on the evolution of a finite beach in a semi-bypassed compartment. The authors here address the problem related to the presence of very short groins, which allow a significant amount of sand to enter or exit the compartment yet from the earliest evolution time steps. It is imperative for the outcrop to be sufficiently long to prevent significant littoral transport during the early simulation stages. Failure to meet this criterion may lead to inconsistencies in the analytical solution.

Then, a further analysis on the bypassed compartment solution was achieved, and a reliability field has been detected on the base of the length of the bypassing groin. The M(t) of a symmetric rectangular beach fill has been derived for the bypassed groin compartment and the decaying process has been then compared to that of the insulated beach, in order to check the effect of bypass on the beach fill evolution. Then, useful design tools for engineers for the calculation of the characteristic reduction times, t^*_{50} and t^*_{25} based on curve fitting analysis, are given.

The further analysis implemented here for the bypassed compartment represents for sure a main point of novelty in literature, together with the check of a reliability range of the solution as a function of the bypass rate of the compartment (i.e. the shortness of the bounding groin).

It is worth noticing that the advantage of using the proposed approach relies in the simplicity of the mathematical problem, making it easier to use compared to other analytical models based on one-line equation, which by contrast need further numerical integration. The absolute generality of the model is also evident in its ability to account for structures at the boundaries of the computational domain of any length, so defining sedimentary cells of various natures.

Despite they can find application in various engineering contexts, main advantage of the proposed analytical tools lies in the initial levels of coastal management projects. As known, coastal projects typically involve multiple technical design phases, such as pre-design, design, monitoring, and evaluation. During the pre-design phase, the objective is to identify and evaluate potential project alternatives using minimal

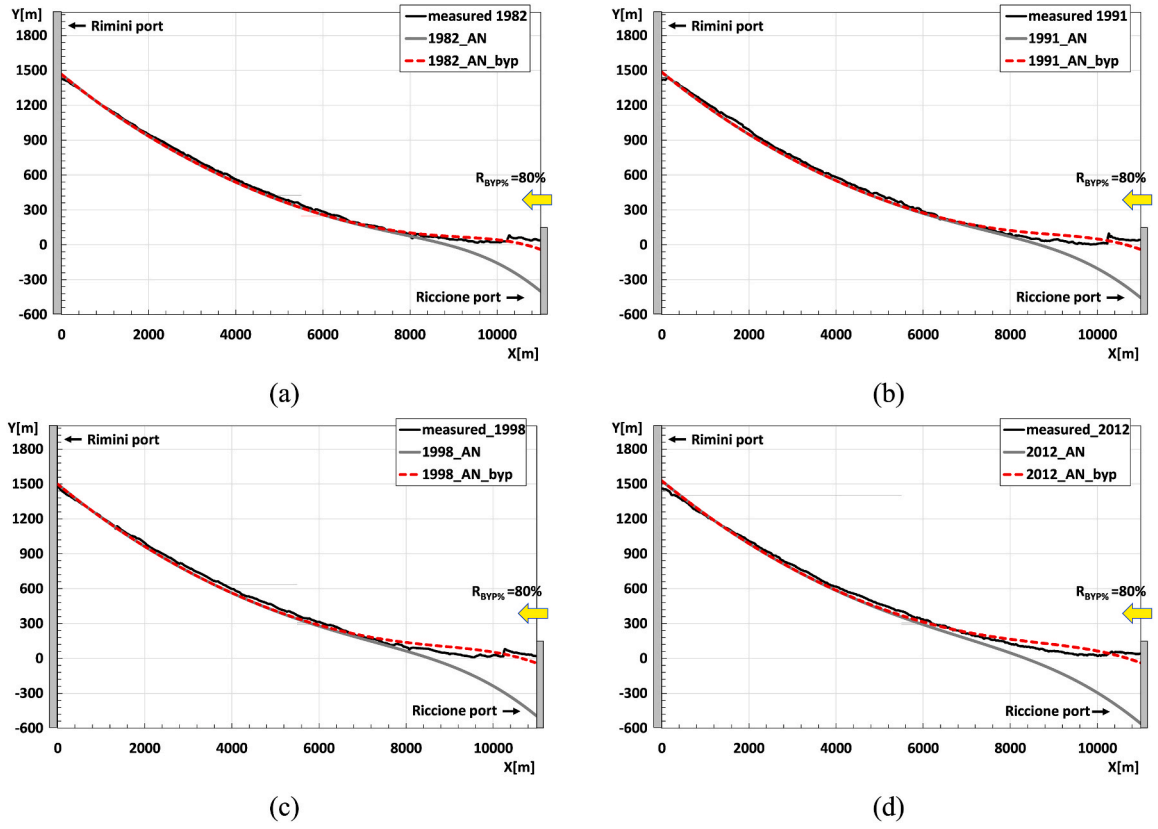

Fig. 17. Comparison of the analytical solution, Eq. (6), - solid grey line of panels (a), (b), (c) and (d) - and the positive heavy-side step solution of Eq. (20) added with the insulated beach solution with the general trend of the Romagna coast - dashed red line of panels (a), (b), (c) and (d). Panel (a) 1982. Panel (b) 1991. Panel (c) 1998. Panel (d) 2012.

input data and employing simple, relatively rapid, and cost-effective methods, as well as low-cost numerical tools. At this preliminary stage, main aim is simply to better define the problem, gain a deeper understanding of the predominant processes, and address initial questions. Consequently, effects of structures within the domain, non-uniform sediment properties, sea level changes, sediment availability, or nonlinear effects like sediment sorting and wave-current interactions are not needed. Therefore, our analytical tools are extremely suitable for the pre-design phases, assisting in reconnaissance and feasibility studies.

Once an alternative is selected, the preliminary design is then refined, and more detailed and comprehensive predictive procedures, numerical tools, and elaborate input data are needed. Such funnel steps facilitate rapid convergence toward the final design solution.

In particular, since these solutions are intended to aid engineers at the early stages of the conceptual design, variational climatic forcings are not directly included in the model. However, two aspects deserve to be considered, and namely:

1) DSE is a linear differential equation, so time-varying wave climate could be modelled as several steps of constant forcings (e.g. monthly climatic steps, then cumulating their effects on the shoreline;
2) It can be observed that in a relatively long time, the effects of the directional spreading of waves about a mean direction, say α_{med}, tend to dampen progressively. We can show that mathematically.

Let us consider a coast of length of l, bounded by two pinned points, for which shoreline position $y(x,t)$ do not move over time. This implies no interruption on the long-shore sediment transport, and the along-shore littoral gradient constant over time. Mathematically, the pinned boundary conditions for the problem here analysed give rise to a Dirichlet problem, which scope is finding a function that satisfies a certain partial differential equation (PDE), that for us is the diffusion equation Eq (2).

The general solution of a Dirichlet problem is:

$$y(x,t) = \sum_{n=1}^{\infty} A_{0n} e^{-\left(\frac{n\pi}{l}\right)^2 \varepsilon} \operatorname{sen}\left(\frac{n\pi}{l} x\right) \tag{29}$$

For more details the reader is referred to Ciccaglione et al. (2023) article.

However, here we assume the diffusion coefficient $\varepsilon(t)$ to be a function of time since the wave angle $\alpha(t)$ and wave height $H(t)$ can vary over a long period for a deep-water wave climate (e.g. with a seasonal or monthly frequency). Considering the Walton and Dean (2010) approach of modelling the diffusivity coefficient ε, the shoreline diffusion can be written as, in terms of deep-water waves:

$$\varepsilon = \frac{1}{D_c + B} \frac{K \bullet (H_0(t))^{2.4} \bullet (T_p)^{0.2} \bullet g^{0.6}}{8 \bullet (s-1) \bullet (1-n) \bullet \pi^{0.2} \bullet \gamma^{0.4} \bullet 2^{1.4}} \bullet \cos(2(\beta - \alpha_0(t))) \tag{30}$$

Now, wave height and wave direction can be seen as harmonic functions of time, $H_0(t)$ and $\alpha_0(t)$ in the form:

$$\alpha_0(t) = B \cos(\sigma_{\alpha_0} t) \tag{31}$$

$$H_0(t) = A \cos(\sigma_{H_0} t) \tag{32}$$

Where σ_{α_0} and σ_{H_0} are the two frequencies of variation of wave height and direction, respectively, while B and A are the amplitude of the harmonic functions.

Accordingly, diffusion can be modelled as the product of two cosine functions, accounting for two different frequencies, σ_{H_0} and σ_{α_0}.Taking this into account, we obtain a $\varepsilon(t)$ function in the form:

$$\varepsilon(t) = \varepsilon_0 + A_0 \cos^m(\sigma_{H_0} t)\cos(\sigma_{\alpha_0} t) \tag{33}$$

Particularly, the cosine function simulating the wave height time variation is raised to a coefficient m, which ranges between 2 and 3 according to the H_0 power of the CERC formula and of Van Rijn's (2014) formula.

Therefore, the general solution of the problem turns into:

$$y(x,t) = \sum_{n=1}^{\infty} A_{0n} e^{-\left(\frac{n\pi}{l}\right)^2 f_\varepsilon} \operatorname{sen}\left(\frac{n\pi}{l}x\right) \tag{34}$$

Where f_ε is a primitive of $\varepsilon(t)$, such that $\frac{\partial f}{\partial t} = \varepsilon_0$, and $\varepsilon(t)$ is the known function of Eq (6.8), while the coefficients: $A_{0n} = \frac{2}{l}\int_0^l f(x)\operatorname{sen}\left(\frac{n\pi}{l}x\right)dx$. By considering an m-coefficient of 3 in Eq. (6.8), the primitive function reads:

$$f_\varepsilon = \varepsilon_0 t + \frac{A_0}{\sigma}\frac{1}{8}\left(\frac{3\sin\left(t\left(\sigma_{H_0} - \sigma_{\alpha_0}\right)\right)}{\sigma_{H_0} - \sigma_{\alpha_0}} + \frac{\sin\left(t\left(3\sigma_{H_0} - \sigma_{\alpha_0}\right)\right)}{3\sigma_{H_0} - \sigma_{\alpha_0}} + \frac{3\sin\left(t\left(\sigma_{H_0} + \sigma_{\alpha_0}\right)\right)}{\sigma_{H_0} + \sigma_{\alpha_0}} + \frac{\sin\left(t\left(3\sigma_{H_0} + \sigma_{\alpha_0}\right)\right)}{3\sigma_{H_0} + \sigma_{\alpha_0}}\right) \tag{35}$$

As far as the two frequencies of wave height and angle are concerned, it is possible that the two frequencies have the same order of magnitude, $\sigma_{H_0} \cong \sigma_{\alpha_0}$, so that both the wave height and direction can change on the same time scale (e.g. bimodal wave conditions). In this case, the general solution becomes:

$$y(x,t) = \sum_{n=1}^{\infty} A_{0n} e^{-\left(\frac{n\pi}{l}\right)^2 \left(\varepsilon_0 + \frac{A_0}{\sigma t}\frac{1}{8}\left(\frac{3\sin\left(t\left(\sigma_{H_0} - \sigma_{\alpha_0}\right)\right)}{\sigma_{H_0} - \sigma_{\alpha_0}} + \frac{\sin\left(t\left(3\sigma_{H_0} - \sigma_{\alpha_0}\right)\right)}{3\sigma_{H_0} - \sigma_{\alpha_0}} + \frac{3\sin\left(t\left(\sigma_{H_0} + \sigma_{\alpha_0}\right)\right)}{\sigma_{H_0} + \sigma_{\alpha_0}} + \frac{\sin\left(t\left(3\sigma_{H_0} + \sigma_{\alpha_0}\right)\right)}{3\sigma_{H_0} + \sigma_{\alpha_0}}\right)\right)t} \bullet \operatorname{sen}\left(\frac{n\pi}{l}x\right) \quad \text{for} \quad \sigma_{H_0} \cong \sigma_{\alpha_0} \tag{36}$$

It is seen that, as t increases, the term $\frac{A_0}{\sigma t}$ becomes even smaller and the diffusivity tends to a constant value ε_0; in other words, this is to say that the shoreline evolution in the long run is led by a constant diffusion, while the time varying diffusivity extra-effect tends to cancel over time. The same result is obtained for $\sigma_{H_0} \gg \sigma_{\alpha_0}$ or $\sigma_{H_0} \ll \sigma_{\alpha_0}$.

The authors verified the above argument empirically by means of the case of Molise coast (Ciccaglione et al., 2021), which is paradigmatic due to its exposition to the bimodal climate of the Adriatic Sea. The inherent bimodality of wave climate makes wave height and, particularly, wave direction to vary over time with a certain frequency. Actually, results showed that even if the beach is expected to "spread heat" as a function of time, the time varying diffusivity extra effect is seen negligible, and shoreline evolution is led by a constant diffusion over a long period.

Additionally, the novel contribution of present paper concerning strongly bypassing compartments enhances the model's adaptability to different conditions without compromising its ease of use.

In fact, authors provide a physically consistent solution, although not rigorously exact, to account for shorter outcrops that allow bypass yet from the first instant of evolution. Despite its mathematical simplicity, achieved by adding some "convective terms" to the diffusive one, the approximate solution is able to fix the early bypass process for both entering/exiting sand flow. It is grounded on the response of an unbounded domain to a positive/negative Heaviside step function, respectively.

The approximated solution proved to be surprisingly suitable to model the early bypass process; a fair agreement was, in fact, detected for the case study of Romagna coast. The 11 km long cell included between Rimini and Riccione ports, experiences an entering bypass process, due to more frequent waves propagating from 60°N. Surprisingly, the positive heavy-side step solution of Eq. (20), added to Eq. (6) is in fair agreement with the beach response, considering an average bypass coefficient, $R_{BYP\%}$, of 80%. The authors found the latter $R_{BYP\%}$ value consistent with the real evolution of the shoreline. Bypass rate can fluctuate from a maximum of 1 (indicating complete bypassing of the groin) to a minimum of zero (indicating the groin extends to the depth of closure, effectively blocking sand transport across the active beach profile). However, for design considerations, it is expected that the groin will block a substantial portion of longshore sediment transport while also allowing for an average bypassing rate (typically engineers set this rate to 30%) to mitigate downdrift effects (Basco and Pope, 2004). For the case of Rimini-Riccione groin cell, the Riccione jetty weakly acts on the sediment flow, allowing significant bypass; this is corroborated by the frequent and significant siltation of the port mouth (Arpae, 2016).

Despite the authors here specifically focused on the coastal stretch between the ports of Rimini and Riccione, where a semi-bypassing compartment scenario with inward flow occurs, it would have been interesting, of course, to test the complementary solution, namely outward flow from the domain, considering the stretch between Cattolica and the port of Riccione. Nevertheless, the southernmost part of the reference physiographic unit, unlike the stretch between Rimini and Riccione, has been heavily modified by human activity, including the construction of coastal defence structures (such as breakwaters and groins) as well as repeated artificial beach fills. This modification makes the comparison of the actual evolution of the examined stretch with the analytical solution quite uncertain.

Although we haven't had the opportunity to discuss the compartment case concerning the outgoing bypass from the domain for the Emilia-Romagna coast; encouraging results will soon be presented in an upcoming article. This article will shift its focus to another case study: the Molise coast, which also faces the Adriatic Sea. Specifically, the authors will examine the response of a 350-m-long groin compartment at the Trigno river mouth, employing the approximated solution for bypass. The results suggest the potential effectiveness of the bypass solution in different coastal scenarios, indicating the need for further investigation and validation.

5. Conclusion

This study delves into the evolution of shoreline in a semi-bypassed compartment using analytical solutions of the one-line model, building upon the work of Ciccaglione et al. (2023). A key challenge lies in ensuring the outcrop length is sufficient to prevent early littoral transport, maintaining consistency in the analytical solution. The paper aims to enhance the general applicability of theoretical results, addressing limitations identified in previous research. By analysing bypassed compartment solutions and deriving M(t) for a symmetric rectangular beach fill, the study assesses the impact of bypass on beach fill evolution. Engineers are provided with useful design tools for calculating characteristic reduction times. Additionally, the authors propose a physically consistent yet approximate solution to account for shorter outcrops allowing bypass from the early steps of evolution. Despite its lack of mathematical rigor, the approximate solution effectively models early bypass processes, showing promising agreement with case studies such as the Romagna coast.

In conclusion, the generalised and rapid-result capacity provided by the proposed theoretical tools turns them into an important aid for stakeholders, such as coastal engineers and planners, for improving coastal adaptation measures and community resilience, as well as for wisely investing economic resources for coastal zone management.

CRediT authorship contribution statement

Margherita Carmen Ciccaglione: Writing – review & editing, Writing – original draft, Software, Investigation, Data curation. **Mariano Buccino:** Writing – review & editing, Validation, Methodology, Investigation, Conceptualization. **Mario Calabrese:** Writing – review & editing, Visualization, Supervision, Formal analysis.

Declaration of competing interest

The authors declare that they have no known competing financial interests or personal relationships that could have appeared to influence the work reported in this paper.

Data availability

The data that has been used is confidential.

APPENDIX 1. Calibration of the transport coefficient K

The calibration of the transport parameter K has been conducted via the OLCE numerical model GENESIS (Hanson and Kraus, 1989). The approach consists in achieving a reasonable consistency between the littoral drift distribution generated by the model (e.g. by the value of the K parameter) and that inferred from the volumetric analyses described in Section 3.3.1.

Particularly, the stretch of coast to be modelled extends for about 14 km between the Port of Rimini up to the last detached breakwater of Misano Adriatica (Fig. 18). The two limits of the domain are intended to totally block the littoral transport; therefore, two "gates" boundary conditions have been set in the numerical model.

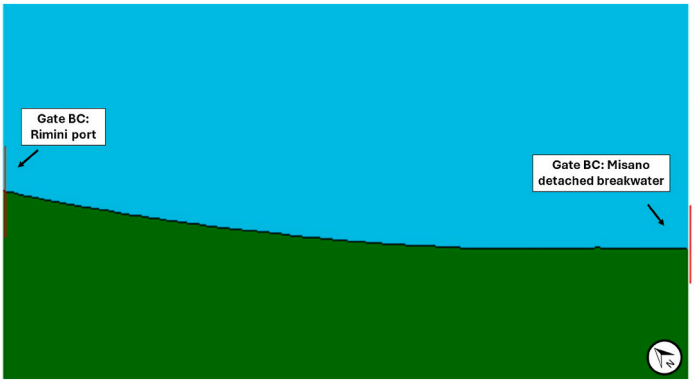

Fig. 18. Initial shoreline and lateral boundary conditions for the GENESIS modelling of the entire stretch from Misano to Rimini.

For the calibration purposes, the port of Riccione is not modelled, as it is considered to only produce a local disturbance (accumulation on the updrift side, erosion on the downdrift side) of limited dimensions compared to the overall extent of the area.

Other constrains of the numerical model are summed up in the following points:

1) The initial configuration of the shoreline is that derived from the 2006 shoreline survey of the Arpae, 2016 study;
2) Grain size of the seabed material, assumed uniform over the entire domain: $d_{50} = 0.17$ mm;
3) The value of the closure depth Dc has been set at 7 m, while the value of the berm height B has been assumed to be 1 m, as mentioned in Section 3.3.;
4) The wave conditions used are the equivalent ones derived from the analysis of the Littoral Drift Rose discussed in Section 3.3. (see Fig. 14), with: $H_{s,eq} = 0.80$ m; $T_{p,eq} = 5$ s; $\alpha_{0,eq} = 60°$N. The aforementioned wave parameters are applied at a depth of 9 m.

The graph in Fig. 19 indicates that a value of K equal to 0.05 closely follows the trend of the northern littoral drift, but fails to reach the peak transport value. Conversely, a value of 0.07 exhibits a different pattern compared to the Arpae study conducted from 2006 to 2012, yet it aligns closely with the peak flow rate value. Consequently, a K transport coefficient of the order of 0.1 has been cautiously chosen.

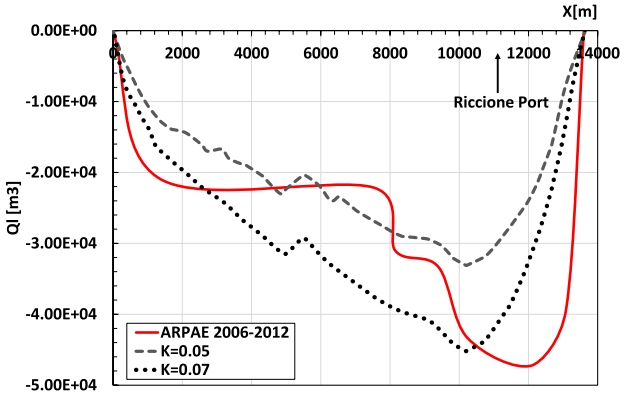

Fig. 19. Comparison of the estimated littoral drift trends with those calculated numerically using K = 0.05 and K = 0.07.

References

Ashton, A.D., Murray, A.B., 2006a. High-angle wave instability and emergent shoreline shapes: 1. Modeling of sand waves, flying spits, and capes. J. Geophys. Res. 111, F04011 https://doi.org/10.1029/2005JF000422.

Ashton, A.D., Murray, A.B., 2006b. High-angle wave instability and emergent shoreline shapes: 2. Wave climate analysis and comparisons to nature. J. Geophys. Res. 111, F04012 https://doi.org/10.1029/2005JF000423.

Basco, D.R., Pope, J., 2004. Groin functional design guidance from the coastal engineering manual. J. Coast Res. (spec. issue 33), 121–130.

Bruun, P., 1954. Coast Erosion and the Development of Beach Profiles, Technical Memorandum No. 44, Beach Erosion Board. US Army Corps of Engineers, Waterways Experiment Station, Vicksburg, MS.

Buccino, M., Del Vita, I., Calabrese, M., 2013. Predicting wave transmission past Reef Ball™ submerged breakwaters. J. Coast Res. (spec. issue 65), 171–176.

Buccino, M., Di Paola, G., Ciccaglione, M.C., Del Giudice, G., Rosskopf, C.M., 2020a. A medium-term study of Molise coast evolution based on the one-line equation and "equivalent wave" concept. Water 12, 2831. https://doi.org/10.3390/w12102831.

Buccino, M., Ciccaglione, M.C., Di Paola, G., 2020b. The use of one-line model and littoral drift rose concept in predicting long term evolution of the Molise coast. In: Proceedings of the Coastal Engineering Conference 36 (ICCE). https://doi.org/10.9753/icce.v36v.sediment.44.

Buccino, M., Ciccaglione, M.C., Di Paola, G., Calabrese, M., 2020c. The use of one-line model and littoral drift rose concepts in predicting long term evolution of the Molise coast. In: Proceedings of the International Offshore and Polar Engineering Conference (ISOPE), pp. 2841–2847.

Carslaw, H.S., Jaeger, J.C., 1959. Conduction of Heat in Solids. Clarendon Press, Oxford.

Ciccaglione, M.C., Buccino, M., Di Paola, G., Calabrese, M., 2021. Trigno River mouth evolution via littoral drift rose. Water (Switzerland) 13 (21), 2995. https://doi.org/10.3390/w13212995.

Ciccaglione, M.C., Buccino, M., Calabrese, M., 2023. On the evolution of beaches of finite length. Continent. Shelf Res. 259, 104990 https://doi.org/10.1016/j.csr.2023.104990. ISSN 0278-4343.

CUGRI - Consorzio inter-Universitario per la previsione e prevenzione dei GRandi rIschi, 2018. Il possibile impatto di barriere sommerse sul litorale romagnolo tra Misano Adriatico e Rimini, REPORT TECNICO.

Dean, R.G., 1977. Equilibrium Beach Profiles: U.S. Atlantic and Gulf Coasts, Ocean Engineering Report No. 12, Department of Civil Engineering. University of Delaware, Newark, DE.

Dean, R.G., 2003. Beach Nourishment — Theory and Practice. World Scientific, Singapore. https://doi.org/10.1142/2160.

Di Paola, G., Ciccaglione, M.C., Buccino, M., Rosskopf, C.M., 2020. Influence of hard defence structures on shoreline erosion along Molise coast (southern Italy): a preliminary investigation. Rendiconti online Italia. (ROL) 52, 2–11. https://doi.org/10.3301/ROL.2020.10.

Emilia-Romagna, Arpae, 2016. Stato del litorale emiliano-romagnolo al 2012. Erosione e interventi di difesa. *I quaderni di Arpae*, 978-88-87854-41-1.

Falqués, A., 2003. On the diffusivity in coastline dynamics. Geophys. Res. Lett. 30 https://doi.org/10.1029/2003GL017760.

Falqués, A., Calvete, D., 2005. Large-scale dynamics of sandy coastlines: diffusivity and instability". J. Geophys. Res. 110, C03007.

Hallermeier, R.J., 1981. A profile zonation for seasonal sand beaches from wave climate. Coast. Eng. 4, 253–277. https://doi.org/10.1016/0378-3839(80)90022-8.

Hanson, H., Kraus, N.C., 1989. GENESIS: generalized model for simulating shoreline change, Report 1, Technical reference. U.S. Army Eng. Waterw. Exp. Stn., Coastal Eng. Res. Cent, Vicksburg.

Hanson, H., Larson, M., Kraus, N.C., Gravens, M.B., 2006. Shoreline response to detached breakwaters and tidal current: comparison of numerical and physical models. In: Proceedings of 31st International Coastal Engineering Conference, vol. 3. World Scientific, pp. 630–633. https://doi.org/10.1142/9789812709554_0305, 642.

Hoang, V.C., 2020. Analytical solutions of one-line model to shoreline change on a coast bounded by solid boundaries. Geo Mar. Lett. 41, 42. https://doi.org/10.1007/s00367-021-00714-7.

Huisman, B.J.A., Van Thiel de Vries, J.S.M., Walstra, D.J.R., Roelvink, J.A., Ranasinghe, R., Stive, M.J.F., 2013. Advection and diffusion of shore-attached sand nourishments. Coastal Dynamics.

Kamphuis, J.W., 1991. Incipient wave breaking. Coast. Eng. 15, 185–203. https://doi.org/10.1016/0378-3839(91)90002-X.

Larson, M., Hanson, H., Kraus, N.C., 1987. Analytical Solutions of the One-Line Model of Shoreline Change, Technical Report CERC-87, U.S. Army of Engineer Waterways Experiment Station. Coastal Engineering Research Center.

Larson, M., Hanson, H., Kraus, N.C., 1997. Analytical solutions of one-line model for shoreline change near coastal structures. J. Waterw. Port, Coast. Ocean Eng. 123 (4), 180–191.

Pelnard-Considere, R., 1956. Essai de theorie de l'evolution des formes de rivage en plages de sable et de galets. In: 4th Journees de l'Hydraulique, Les Energies de la Mer, vol. III. La Houille Blanche, Grenoble, France, pp. 289–298.

Reeve, D.E., 2006. Explicit expression for beach response to nonstationary forcing near a groyne. J. Waterw. Port, Coast. Ocean Eng. 132 (2), 125–132. https://doi.org/10.1061/(ASCE)0733-950X(2006)132:2(125).

Reeve, D.E., Valsamidis, A., 2014. On the stability of a class of shoreline planform models. Coast. Eng. 91, 76–83. https://doi.org/10.1016/j.coastaleng.2014.05.005.

Shore Protection Manual (SPM), 1984. U.S. Government Printing Office, Washington D. C.

Valsamidis, A., Reeve, D.E., 2017. Modelling shoreline evolution in the vicinity of a groyne and a river. Continent. Shelf Res. 132, 49–57. https://doi.org/10.1016/j.csr.2016.11.010.

Valsamidis, A., Reeve, D.E., 2020. A new approach to analytical modelling of groin fields. Continent. Shelf Res. 211, 104288 https://doi.org/10.1016/j.csr.2020.104288.

Valsamidis, A., Cai, Y., Reeve, D.E., 2013. Modelling beach-structure interaction using a Heaviside technique: application and validation. J. Coast Res. 410–415. https://doi.org/10.2112/SI65-070.1.

Van Rijn, L.C., 2014. A simple general expression for long-shore transport of sand, gravel and shingle. 513. Coast. Eng. 90, 23–39.

Walton Jr., T.L., 2005. A review of inlet bypassing solutions with nomographs. Coast. Eng. 52, 1127–1132. https://doi.org/10.1016/j.coastaleng.2005.07.003.

Walton, T.L., Dean, R.J., 1973. Application of littoral drift roses to coastal engineering problems. In: Proceedings of the Conference on Engineering Dynamics in the Surf Zone. Institution of Engineers, Sydney, Australia, pp. 221–227, 14–17 May 1973.

Walton, T.L., Dean, R.G., 2010. Long-shore sediment transport via littoral drift rose. Ocean. Eng. 37, 228–235. https://doi.org/10.1016/j.oceaneng.2009.11.002.

Walton Jr, T.L., Dean, R.G., 2011. Shoreline change at an infinite jetty for wave time series. Continent. Shelf Res. 31, 1474–1480. https://doi.org/10.1016/j.oceaneng.2009.11.002.

Zacharioudaki, A., Reeve, D.E., 2008. Semi-analytical solutions of shoreline response to time varying wave conditions. J. Waterw. Port, Coast. Ocean Eng. 134, 265–274. https://doi.org/10.1061/(ASCE)0733-950X(2008)134:5(265).